Supporting Information for

Pillar[5]arene-based ionic single crystals formed by dual self-assemblies through host-guest and ionic interactions for iodine capture

Ting Zhang[a,b,#], Lulu Wang[b,#], Hui Li[a], Mingxia Sun[a], Jia Chen[a*], Shuzhe Guan[b*] and Hongdeng Qiu[a,c*]

[a] CAS Key Laboratory of Chemistry of Northwestern Plant Resources and Key Laboratory for Natural Medicine of Gansu Province, Lanzhou Institute of Chemical Physics, Chinese Academy of Sciences, Lanzhou 730000, China.

[b] State Key Laboratory of Chemistry and Utilization of Carbon Based Energy Resources, College of Chemistry, Xinjiang University, Urumqi 830017, China.

[c] Key Laboratory of Rare Earths, Ganjiang Innovation Academy, Chinese Academy of Sciences, Ganzhou 341000, China.

[#] These two authors contributed equally.

*Corresponding Authors: jiachen@licp.cas.cn (J. Chen); 254425698@qq.com (S. Guan); hdqiu@licp.cas.cn (H. Qiu).

Table of Contents

1. Materials and methods

Materials: Unless otherwise specified, all chemicals were of analytical grade and were not further purified. Petroleum ether, methylene chloride, ethyl acetate, and acetonitrile were purchased from Damao Chemical Reagent (Tianjin, China). Toluene and ethanol were purchased from Xilong Scientific. $BF_3 \cdot OEt_2$ was purchased from Saen Chemistry Technology Co., Ltd. (Shanghai, China). 1, 4-di-bromobutane, dimethylhydroquinone, paraformaldehyde, and 1, 4-dimethoxybenzene were purchased from Energy Chemical. 1-methylimidazole and 1, 2-dichloroethane were purchased from Chengdu Chron Chemicals. K_2CO_3 was provided by Shanghai Chemical Reagent Company of China Pharmaceutical Group (Shanghai, China). Iodine and 1, 5-naphthalenedisulfonic acid were purchased from Shanghai Aladdin Biochemical Technology Co., Ltd. (Shanghai, China).

Methods: The ^{1}H nuclear magnetic resonance (^{1}H NMR) and ^{13}C nuclear magnetic resonance (^{13}C NMR) spectra were measured on the AVANCE III HD 400 MHz nuclear magnetic resonance spectrometer (Bruker, Switzerland). Thermogravimetric analysis (TGA) was determined by a STA449F3 simultaneous thermal analyzer (Netzsch, Germany). X-ray diffraction (XRD) was carried out on the LabX XRD-6100 (Shimadzu, Japan). The Fourier Transform Infrared Spectroscopy (FT-IR) results were collected using a Vertex 70v FT-IR Spectrometer (Bruker, Germany). Raman spectroscopy was performed on a confocal microscope (Renishaw, U.K.). X-ray photoelectron spectroscopy (XPS) was collected using an ESCALAB 250Xi photoelectron spectrometer (ThermoFisher Scientific, USA). The Brunauer-Emmett-Teller (BET) surface area and pore size were detected by a fully automated specific surface and porosity analyzer (Micromeritics ASAP 2460, USA). X-ray crystallography was collected using a Smart APEX II X-ray single-crystal diffractometer (Bruker, Germany). The absorbance of I_2 was measured on a UV-3600plus UV-visible spectrophotometer (UV-Vis) (Shimadzu Corporation, Japan).

2. Synthesis and characterization

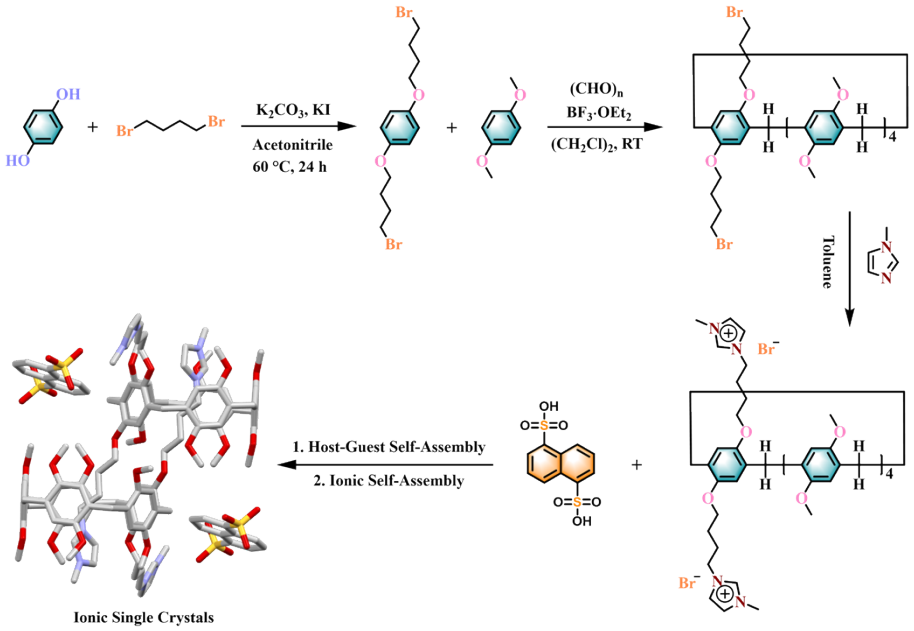

Scheme S1 Synthetic route to ionic single crystals (DMIBP5-NA).

Preparation of 1,4-bis(2-bromo-butoxy)benzene (DBB)

The compounds 1, 4-dibromobutane (8.6 g, 40 mmol), hydroquinone (2.3 g, 20 mmol), and the catalysts K_2CO_3 (16.6 g, 120 mmol) and KI (39.8 g, 120 mmol) were sequentially added to acetonitrile solvent (50 mL) and heated under reflux at 60 °C for 24 h (Fig. S1). After the reaction, the mixture was distilled under reduced pressure. The crude product was purified by column chromatography (petroleum ether/ethyl acetate = 100:1, v/v), yielding compound 1 as a white solid (4.6 g, 60%). The ^{1}H NMR spectrum of compound 1 was shown in Fig. S2: ^{1}H NMR (400 MHz, $CDCl_3$, 298 K), δ (ppm): 6.85 (s, 4H), 3.98 (t, J=4.0 Hz, 4H), 3.52 (t, J=8.0 Hz, 2H), 3.29 (t, J=8.0 Hz, 2H), 2.08 (m, 4H), 1.93 (m, 4H).

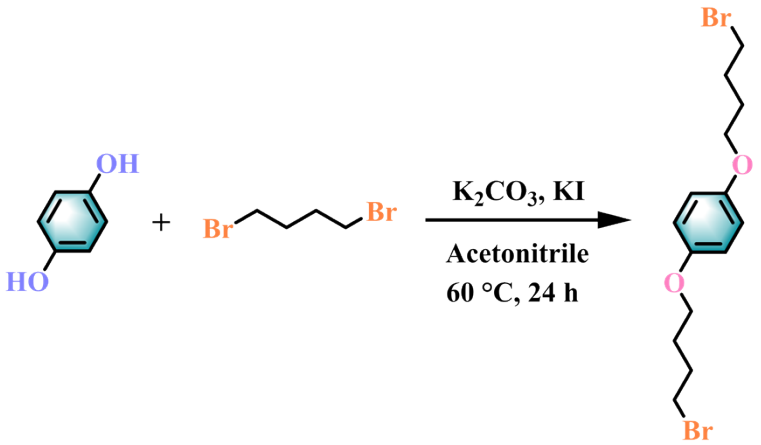

Fig. S1 The synthetic routes to DBB.

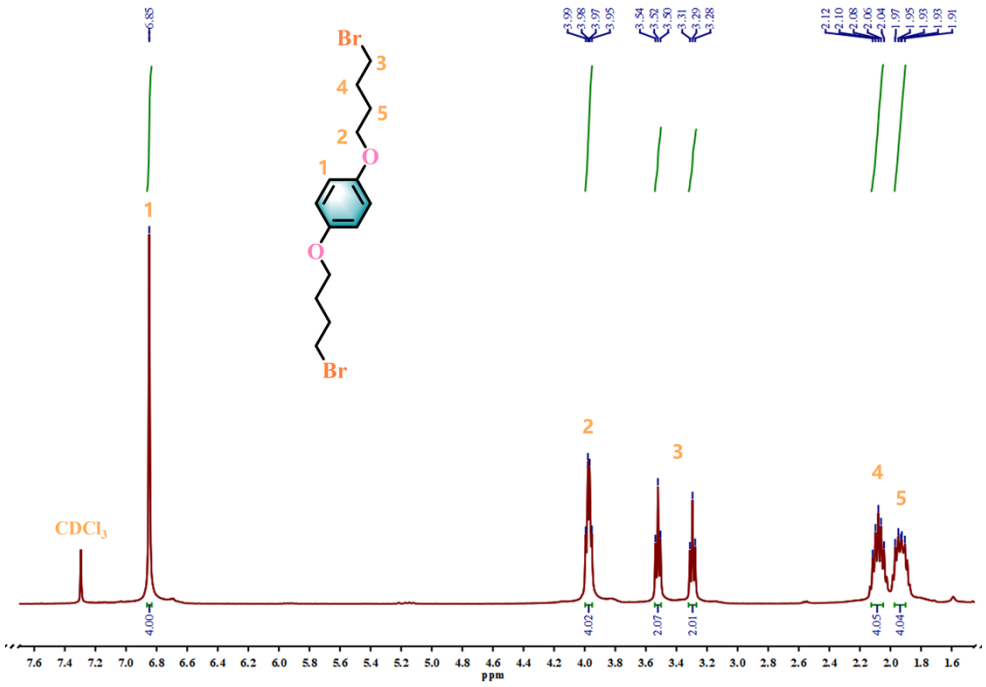

Fig. S2 ^{1}H NMR spectrum (400 MHz, $CDCl_3$, 293 K) of DBB.

Preparation of 1, 4-bis(2-bromo-butoxy)-benzene-pillar[5]arene (DBBP5)

The compounds 1, 4-bis(2-bromo-butoxy)benzene (1) (3.8 g, 10 mmol), 1, 4-dimethoxybenzene (5.5 g, 40 mmol), paraformaldehyde (1.0 g), and $BF_3 \cdot OEt_2$ (1 mL) were sequentially introduced into 1, 2-dichloroethane (200 mL) at room temperature and stirred for 2 h (Fig.S3). After the reaction, the mixture was extracted with dichloromethane. The organic layer was washed with water and dried over Na_2SO_4, and the solvent was evaporated under vacuum. The crude product was purified by column chromatography (petroleum ether/ethyl acetate = 50:1, v/v) to yield compound 2 as a white solid (2.9 g, 29 %). The ^1H NMR spectrum of compound 2 is shown in Fig. S4: ^1H NMR (400 MHz, $CDCl_3$, 298 K), δ (ppm): 6.82-6.72 (m, 10H), 3.77 (s, 14H), 3.68 (t, J = 4.0 Hz, 24H), 3.11 (s, 4H), 1.69 (s, 8H). Fig. S5: ^{13}C NMR (100 MHz, $CDCl_3$, 298 K), δ (ppm): 150.84, 150.79, 150.75, 150.63, 149.89, 128.45, 128.34, 128.29, 128.25, 128.12, 114.95, 114.20, 114.15, 113.99, 113.77, 67.36, 55.97, 55.95, 55.79, 55.73, 33.39, 29.76, 29.56, 29.50, 29.31, 28.35.

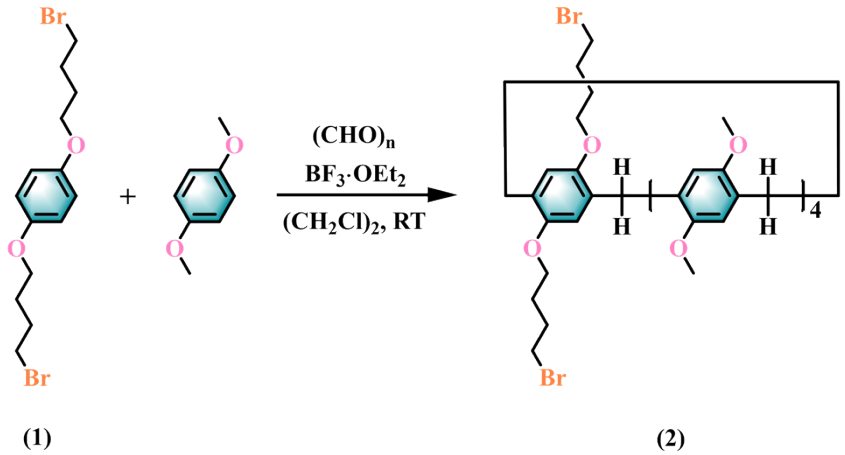

(1) (2)

Fig. S3 The synthetic routes to DBBP5.

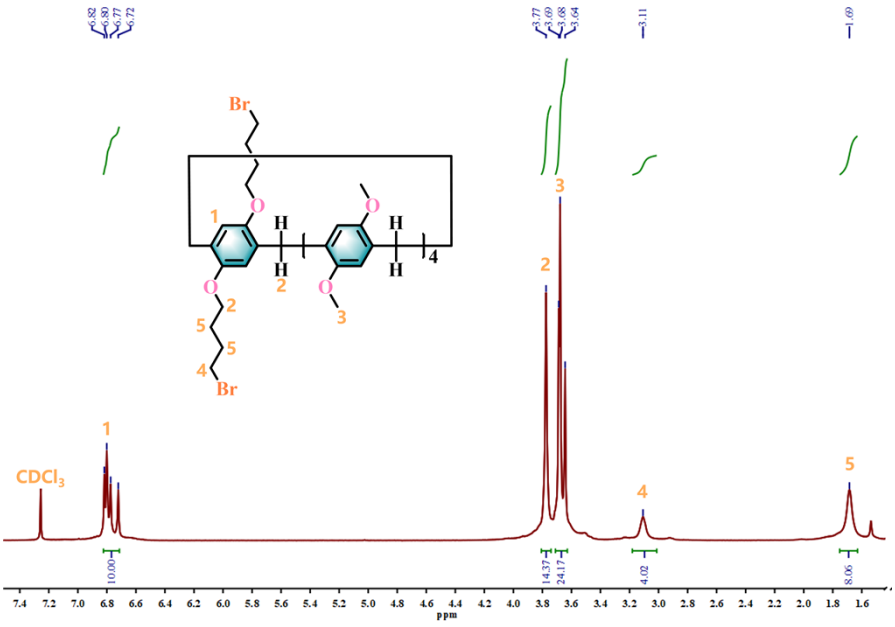

Fig. S4 ^1H NMR spectrum (400 MHz, $CDCl_3$, 293 K) of DBBP5.

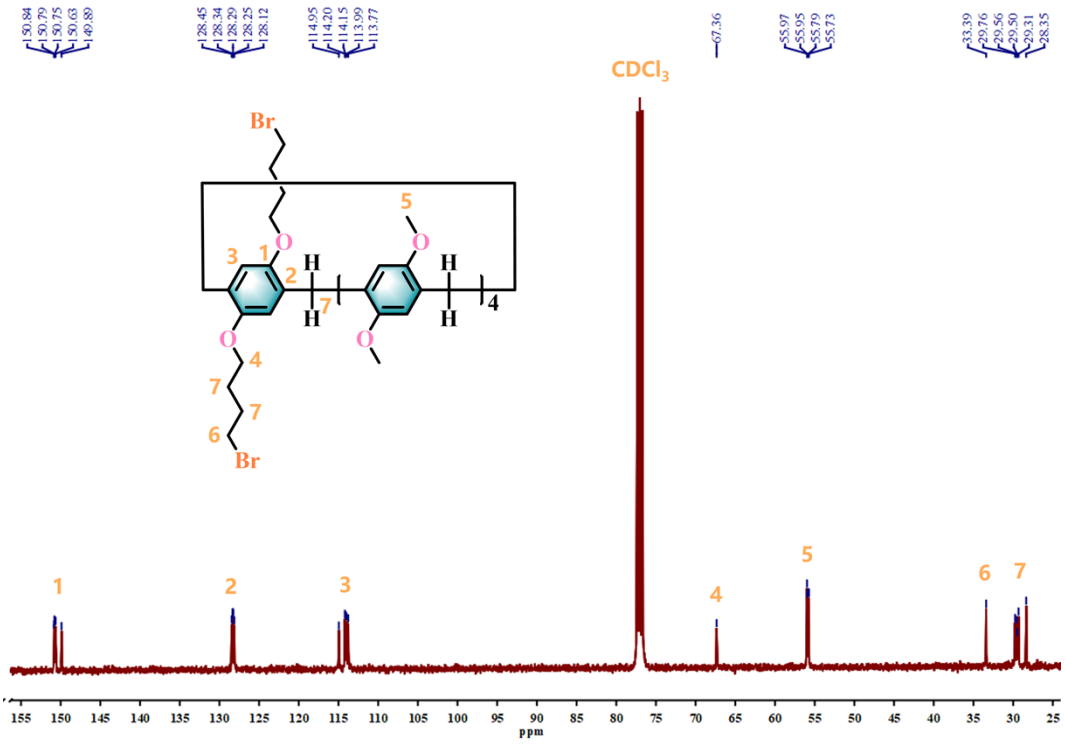

Fig. S5 ^{13}C NMR spectrum (100 MHz, $CDCl_3$, 293 K) of DBBP5.

Preparation of 1, 4-bis(2-methylimidazolium-butoxy)-benzene-pillar[5]arene (DMIBP5)

A mixture of 1, 4-bis(2-bromo-butoxy)-benzene-pillar[5]arene (2) (3.0 g, 3 mmol) and N-methylimidazole (0.5 g, 6 mmol) in toluene was heated under reflux at 80 °C for 5 h. After cooling to 25 °C, the solvent was removed under vacuum. The residue was then recrystallized from a mixture of petroleum ether and dichloromethane (1:1) to afford 2.8 g (92 %) of a white solid (Fig.S6). The ^{1}H NMR spectrum of compound 3 is shown in Fig. S7: ^{1}H NMR (400 MHz, DMSO-d_6, 298K), δ (ppm): 8.84 (s, 2H), 7.80 (s, 2H), 7.51 (s, 2H), 6.79-6.75 (m, 10H), 4.25 (t, J = 8.0 Hz, 4H), 3.86 (t, J = 4.0 Hz, 4H), 3.66 (t, J = 8.0 Hz, 30H), 3.60 (s, 10H), 2.03 (t, J = 8.0 Hz, 4H), 1.74 (t, J = 8.0 Hz, 4H). Fig. S8: ^{13}C NMR (100 MHz, DMSO-d_6, 298K), δ (ppm): 150.06, 150.02, 149.99, 149.15, 136.40, 127.81, 127.79, 127.77, 127.69, 123.59, 122.32, 114.26, 113.54, 113.45, 67.23, 55.74, 55.69, 55.61, 48.76, 35.57, 29.01, 26.48, 25.97.

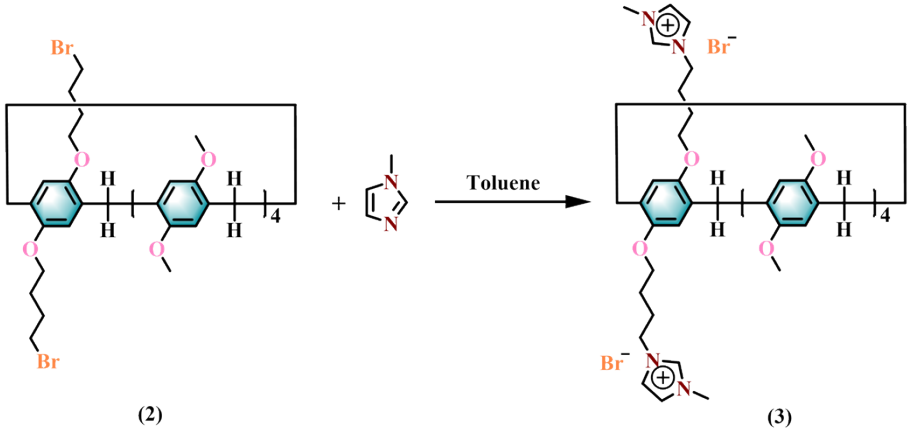

Fig. S6 The synthetic routes to DMIBP5.

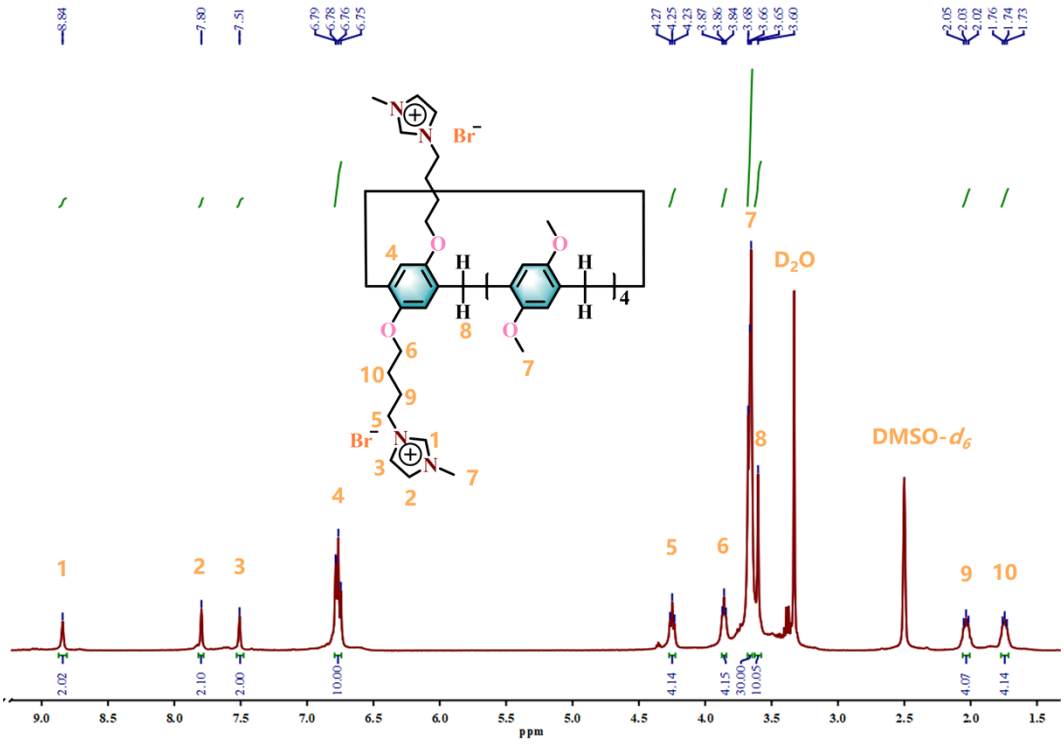

Fig. S7 ^{1}H NMR spectrum (400 MHz, DMSO-d_6, 293 K) of DMIBP5.

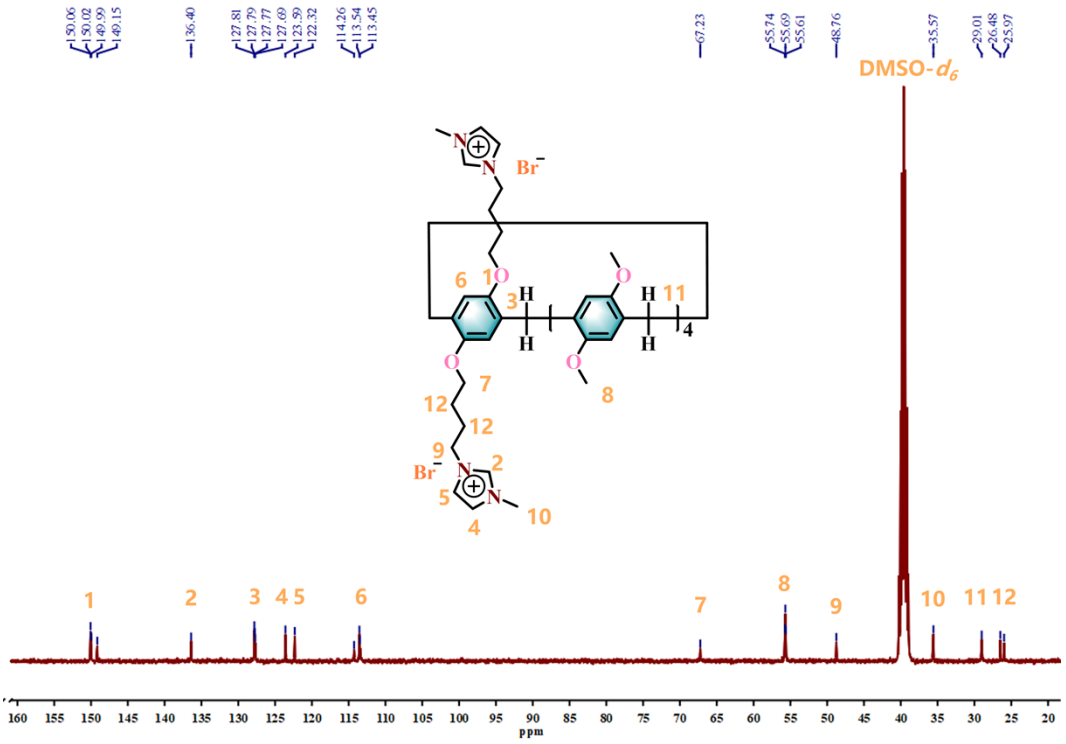

Fig. S8 ^{13}C NMR spectrum (100 MHz, DMSO-d_6, 293 K) of DMIDP5.

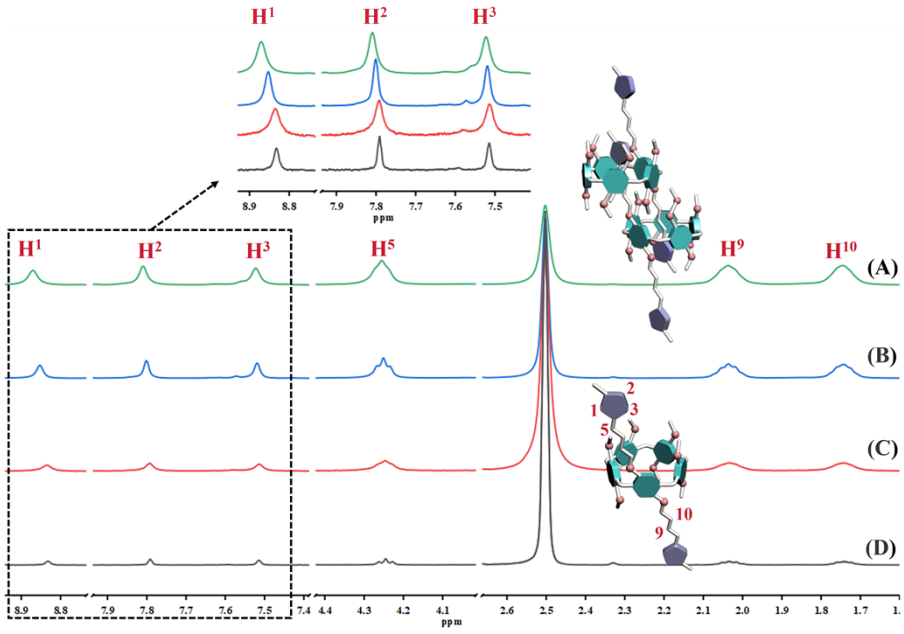

Fig. S9 Partial ^{1}H NMR spectra (400 MHz, DMSO-d_6, 293 K) of DMIBP5 at varying monomer concentrations:

(A) 20.00, (B) 10.00, (C) 3.00, and (D) 1.00 mM.

Preparation of DMIBP5-NA

Equimolar amounts of DMIBP5 and NA were dissolved in ethanol, and the solution was kept at 25 °C for 48 h, yielding pale-yellow crystals.

Table S1 Summary of Crystallographic Data.

	DMIBP5-NA
Formula	$C_{73}H_{90}N_4O_{18}S_2$
CCDC No.	2415287
Formular weight	2567.05 g/mol
Crystal system	triclinic
Space group	P-1
a/Å	13.938(3)
b/Å	16.892(4)
c/Å	18.001(4)
α/°	77.270(4)
β/°	68.987(4)
γ/°	75.532(4)
Volume/Å^3	3790.4(14)
Z	2

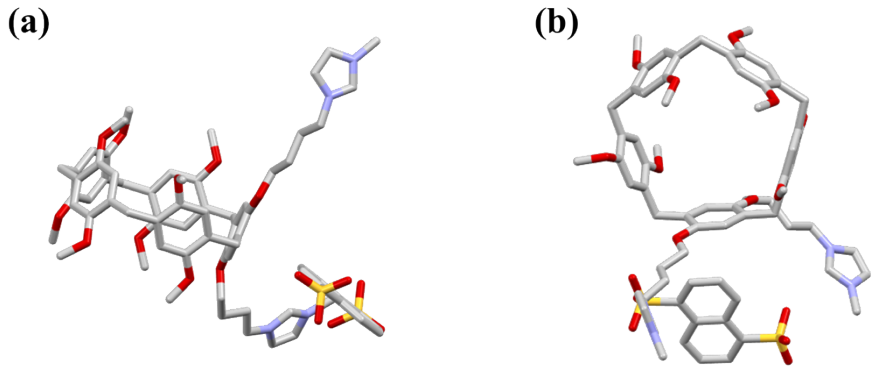

Fig. S10 (a) The asymmetric unit structure of DMIBP5-NA along the a-axis. (b) The asymmetric unit structure of DMIBP5-NA along the c*-axis.

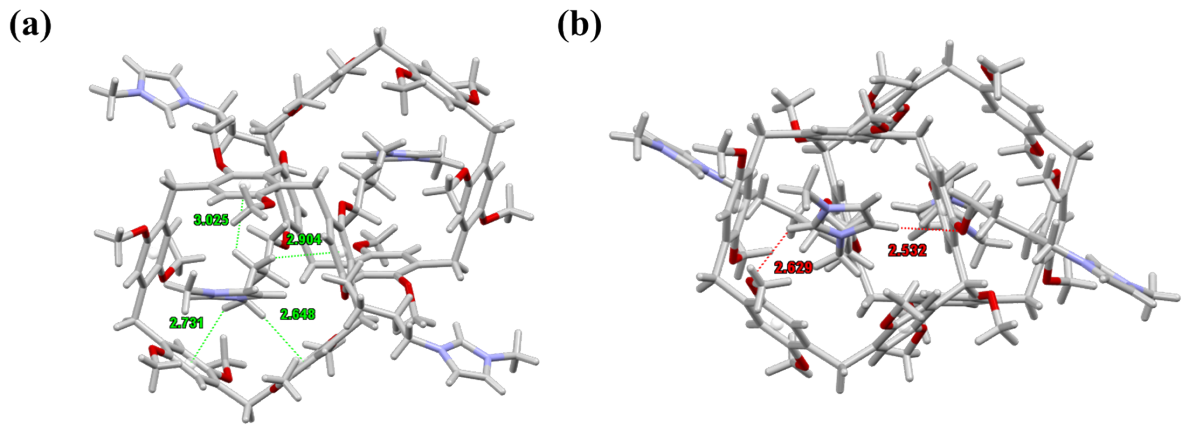

Fig. S11 (a) The green dashed line indicates C-H···π interaction. (b) the red dashed line indicates C-H···O interaction (to highlight the C-H···π and C-H···O interactions, the NA moiety was omitted in the figure).

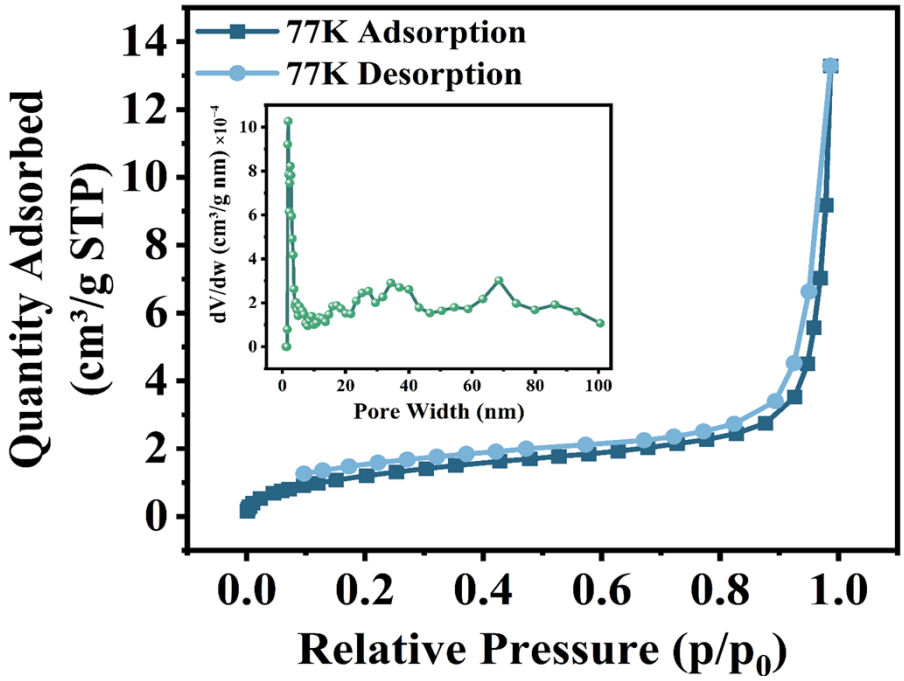

Fig. S12 N_2 sorption isotherms for DMIBP5-NA. Inset: derived pore size distribution profiles for DMIBP5-NA.

3. Experimental section

Iodine adsorption experiment in solution

Initially, a set of iodine-cyclohexane solutions with different concentrations was systematically prepared, and their UV-vis spectra were recorded to establish a calibration curve. Subsequently, DMIBP5-NA was added to a cyclohexane solution containing 25 ppm iodine. The calibration curve was then applied to ascertain the residual iodine concentration in the cyclohexane solution. The Equation S1 for calculating iodine capture [1, 2] (Q_t, mg/g) is as follows:

$$Q_t = \frac{(C_0 - C_t)}{m} V \qquad \text{S(1)}$$

In this formula, C_0 and C_t (mg/L) represent the concentrations of iodine-cyclohexane solutions at zero and t moments, respectively. V (L) represents the volume of the iodine-cyclohexane solutions, while m (g) indicates the weight of DMIBP5-NA.

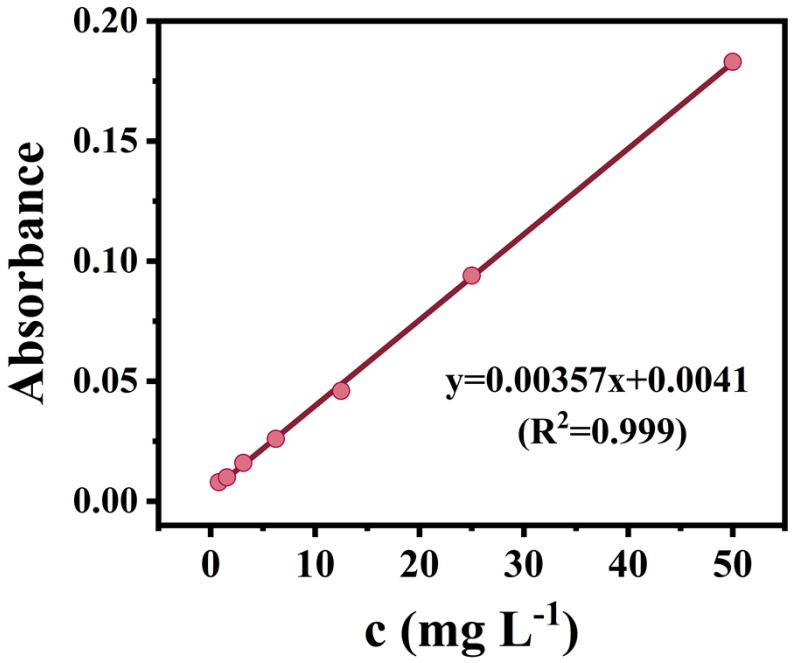

Fig. S13 Linear fit of absorbance values to iodine concentration in cyclohexane solution.

Iodine vapor uptake experiments

The gravimetric method was employed to assess the iodine capture capacity of DMIBP5-NA. DMIBP5-NA and excess iodine were placed in a sealed bottle, ensuring no physical contact was made between the iodine and DMIBP5-NA. The bottle was then stored in a 70 °C oven to capture the iodine. After an appropriate period, remove the sample bottle and position it in a fume hood. Allow it to cool to room temperature to eliminate any free iodine vapor. Subsequently, the sample was weighed at various intervals to document the extent of adsorption over time. This process continued until no further changes in mass were observed. The iodine capture capacity is calculated using Equation S2, where Δm (g) represents the mass gain and m_s (g) represents the initial mass of the sorbent.[3-5] The variable q_e (mg/g) represents the iodine capture capacity of the sorbent.

$$q_e(mg/g) = \frac{\Delta m}{m_s} \times 1000 \qquad \text{S(2)}$$

The adsorption data of iodine vapor by DMIBP5-NA were analyzed using both the pseudo-first-order and pseudo-second-order kinetic models, by fitting Equations S(3) and S(4) [3]. Where k_1 and k_2 represent the corresponding rate constants, t (min) indicates the time. The variables q_e and q_t (mg/g) denote the equilibrium adsorption capacity and the adsorption capacity at time t (min), respectively. Equation S(2) can be used to calculate q_e.

First order fitting: $$\ln (q_e - q_t) = \ln q_e - k_1 t \qquad \text{S(3)}$$

Second order fitting: $$\frac{t}{q_t} = \frac{1}{k_2 q_e^2} + \frac{t}{q_e} \qquad \text{S(4)}$$

Table S2 Comparison of DMIBP5-NA with other absorbents reported in previous studies for iodine adsorption.

Adsorbents	Iodine state	T (℃)	Adsorption capacity (mg/g)	Eq. time	Ref.
P4	I_2(g)	40	3930	42 h	6
SB-PA1	I_2(g)	80	1660	25 h	7
SB-PA2	I_2(g)	80	1780	25 h	
SB-PA3	I_2(g)	80	1660	25 h	
SB-DM	I_2(g)	80	1330	25 h	
EtP6	I_2(g)	85	250	2 h	8
P[5]A-MPP	I_2(g)	80	3840	24 h	9
CMP-1	I_2(g)	75	1510	30 h	10
CMP-2	I_2(g)	75	1770	30 h	
CMP-3	I_2(g)	75	1310	30 h	
CP-4	I_2(g)	75	2080	30 h	
P5-P5I	I_2(g)	75	2130	4 h	11
DMIBP5-NA	I_2(g)	70	3280	48 h	This work

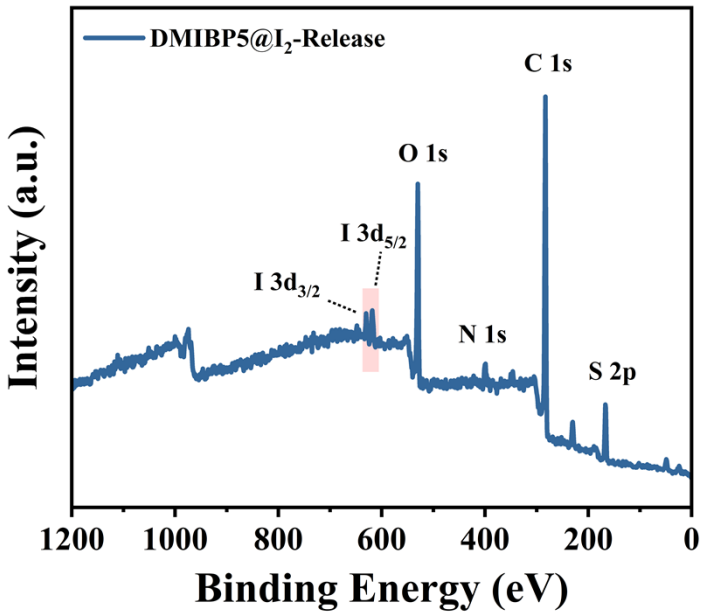

Fig. S14 XPS survey spectra for DMIBP5-NA@I_2 release iodine.

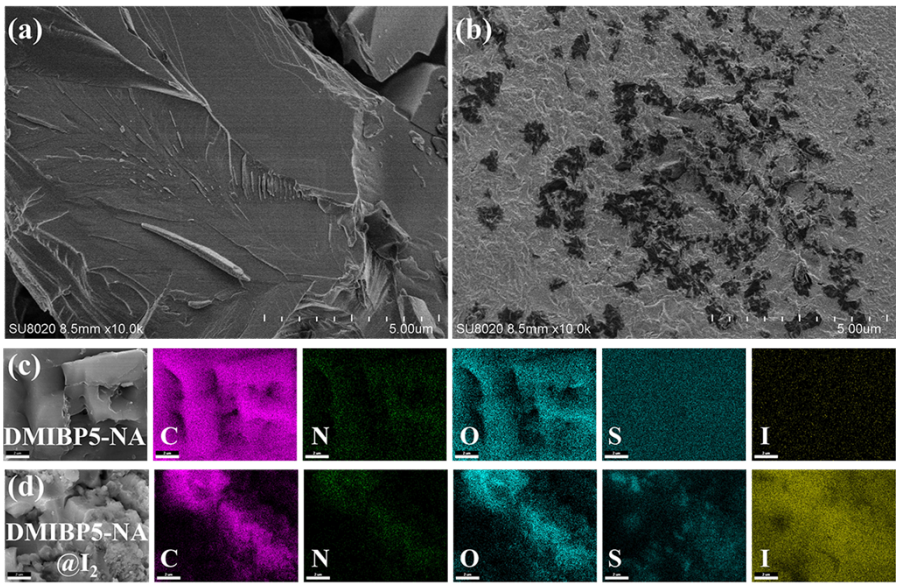

Fig. S15 (a) SEM image of DMIBP5-NA (scale bar: 5.00 μm). (b) SEM image of DMIBP5-NA@I_2 (scale bar: 5.00 μm). (c) Elemental mapping images for DMIBP5-NA (scale bar: 2.5 μm). (d) Elemental mapping images for DMIBP5-NA@I_2 (scale bar: 2.5 μm).

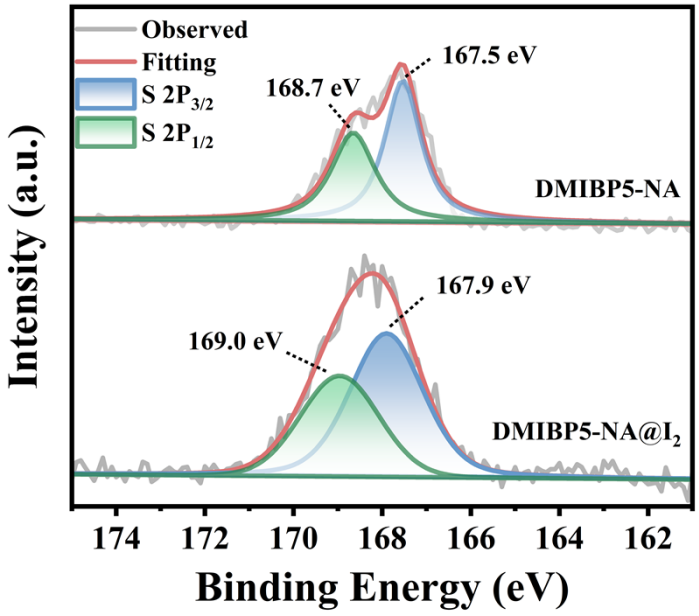

Fig. S16 S 2p XPS spectra for DMIBP5-NA and DMIBP5-NA@I_2.

4. Density functional theory calculations

Based on the [*c*2]daisy chain structural features of pillar[5]arene and considering the influence of cavity steric effects on iodine adsorption performance, this study retained the imidazolyl group configuration within the cavity in DFT calculations.

The calculations were performed using the Vienna ab initio simulation package (VASP 6.2.1)[12-14] and the Perdew-Burke-Ernzerhof form of the Generalized Gradient Approximation (GGA-PBE)[15] functional was employed to obtain the exchange and correlation terms. The DFT-D3(BJ) method of Grimme[16, 17] was used to describe long-range vdW interactions.

The optimization and the calculation were performed with an energy cutoff of 400 eV, using a k-mesh of 1x1x1 and achieving energy and force convergence of 1×10^{-5} eV and 0.02 eV/Å, respectively. the optimized lattice parameters of host are 20.93 Å × 22.16 Å × 18.47 Å with α=77.3°, β=69.0°, γ=75.5°.The charge density difference, denoted as Δρ, is calculated as the difference between the total charge density of the molecules adsorbed on the slab ($\rho_{molecule@slab}$), the charge density of the slab itself (ρ_{slab}), and the charge density of the molecules in the gas phase ($\rho_{molecule}$). This is written mathematically as:

$$\Delta\rho = \rho_{molecule@slab} - \rho_{slab} - \rho_{molecule}$$

The charge transfer between the molecules and the surface can be determined through Bader charge analysis.[18]

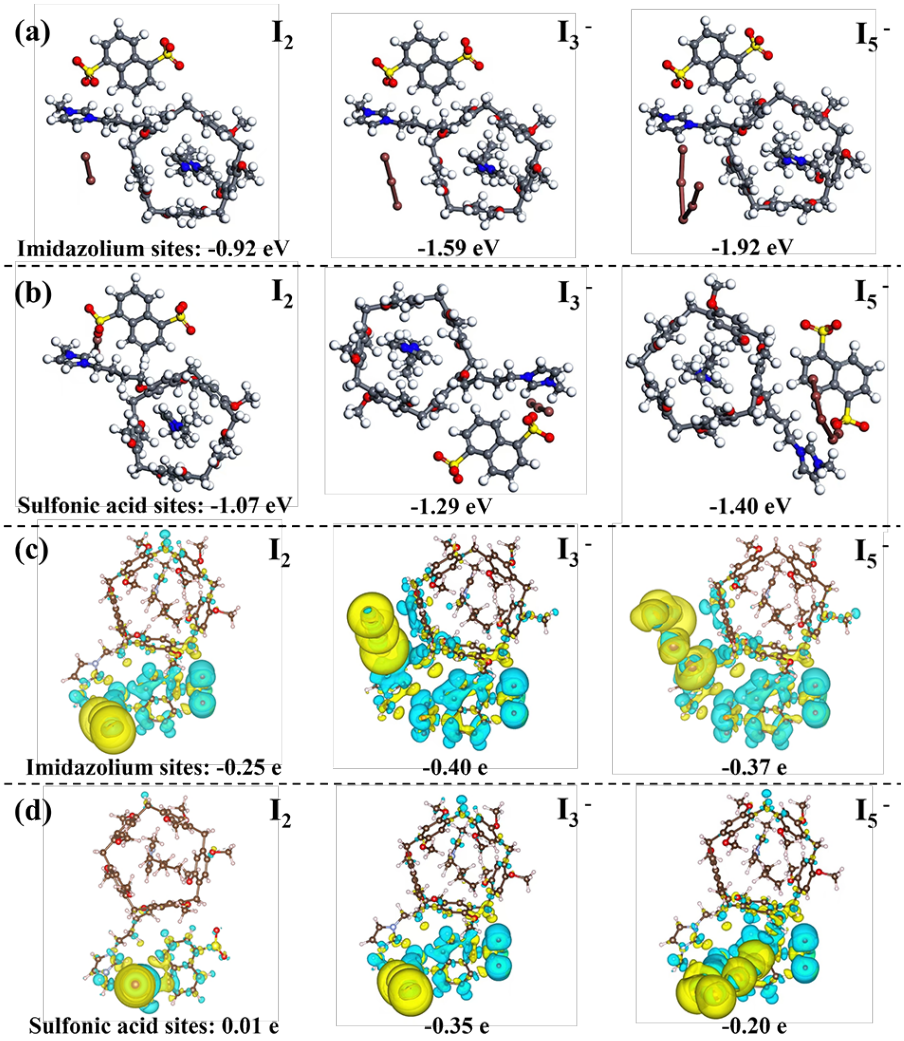

Fig. S17 Structural models and binding energies of I_2, I_3^- and I_5^- ions interacting with (a) imidazolium and (b) sulfonic acid sites. Charge density differences and Bader charge transfers for I_2, I_3^- and I_5^- ions adsorbed onto (c) imidazolium and (d) sulfonic acid sites of DMIBP5-NA.

5. References

1 A. Sen, S. Sharma, S. Dutta, M. M. Shirolkar, G. K. Dam, S. Let and S. K. Ghosh, *ACS Appl. Mater. Interfaces*, 2021, **13**, 34188-34196.

2 J. Wen, F. Hu, B. Liu, H. Chen, M. Yang, Y. Liu and H. Li, *Eur. Polym. J.*, 2023, **201**, 112596.

3 Y. Gao, Y. Huo, M. Chen, X. Su, J. Zhan, L. Wang, F. Liu, J. Zhu, Y. Zeng, J. Fan, Z. Li, R. Chen and H.-L. Wang, *Adv. Fiber Mater.*, 2023, **5**, 1431-1446.

4 M. A. S. Salem, A. M. Khan, Y. K. Manea, M. T. A. Qashqoosh and F. A. M. Alahdal, *J. Hazard. Mater.*, 2023, **447**, 130732.

5 B. Xue, Y. Lv, W. Xuan, W. Zhu, Z. Li, L. Zhang and J.-Q. Wang, *J. Colloid Interface Sci.*, 2025, **692**.

6 Q. Zhang, J. Li, T.-J. Yue, N. Li, Y.-Q. Jiang and H.-M. Guo, *J. Solid State Chem.*, 2024, **331**.

7 S. Srividhya, A. Roja and M. Arunachalam, *ACS Appl. Polym. Mater.*, 2024, **6**, 3470-3480.

8 K. Jie, Y. Zhou, E. Li, Z. Li, R. Zhao and F. Huang, *J. Am. Chem. Soc.*, 2017, **139**, 15320-15323.

9 J. Kiruthika and M. Arunachalam, *Polymer*, 2022, **259**, 125322.

10 D. Dai, J. Yang, Y. C. Zou, J. R. Wu, L. L. Tan, Y. Wang, B. Li, T. Lu, B. Wang and Y. W. Yang, *Angewandte Chemie*, 2021, **133**, 9049-9057.

11 Y. Chen, M.-K. Yang, S.-X. Li, S.-L. Zhou, C.-N. Hu, Y.-H. Yang and L.-J. Yang, *ACS Appl. Mater. Interfaces*, 2025, **17**, 8382-8393.

12 G. Kresse and J. Furthmüller, *Phys. Rev. B*, 1996, **54**, 11169-11186.

13 G. Kresse and J. Furthmüller, *Comput. Mater. Sci.*, 1996, **6**, 15-50.

14 G. Kresse and J. Hafner, *Phys. Rev. B*, 1993, **47**, 558-561.

15 J. P. Perdew, K. Burke and M. Ernzerhof, *Phys. Rev. Lett.*, 1997, **78**, 1396-1396.

16 S. Grimme, S. Ehrlich and L. Goerigk, *J. Comput. Chem.*, 2011, **32**, 1456-1465.

17 G. Henkelman, A. Arnaldsson and H. Jónsson, *Comput. Mater. Sci.*, 2006, **36**, 354-360.

18 W. J. Orville-Thomas, *J. Mol. Struct.:THEOCHEM*, 1996, **360**, 175.